

Supporting Information

Solid-Phase Synthesis of Atomically Thin Two-Dimensional Nonlayered MoO₂ Nanosheets for Surface Enhanced Raman Spectroscopy

Xiangcheng Lin,^{†,#} Pengfei Yan,^{†,#} Fafeng Xu,[‡] Wenzhuo Wu,[†] Tianzhao Hu,[†] Cong Wei,^{,†} Qun Xu,^{*,†}*

[†]College of Materials Science and Engineering, Zhengzhou University, Zhengzhou 450001, China.

[‡]Key Laboratory of Photochemistry, Institute of Chemistry, Chinese Academy of Sciences, Beijing 100190, China.

E-mail: weicong@zzu.edu.cn; qunxu@zzu.edu.cn

Materials and experimental details

1. Materials:

MoO₃ powder was provided by Alfa Aesar. Zinc powder was purchased from Sigma-Aldrich. Ethanol (AR) and ammonia (AR) was purchased from Sinopharm Chemical Reagent Co., Ltd. (China). Deionized water was prepared with double-distilled water.

2. Synthesis of 2D-MoO₂ nanosheets:

In a typical synthesis, 0.5g of molybdenum oxide and 0.01g of zinc powder were added into a mortar and mixed for 30 minutes. And then, add the mixture into a porcelain boat and heat it for 0.5 h at 400°C. After finishing the reaction, the black products were washed sequentially with aqueous ammonia, hydrochloric acid and distilled water for three times. Finally, 2D-MoO₂ nanosheets were collected by centrifugation and dried at 60°C in a vacuum drying oven.

3. Raman measurement:

In order to evaluate the SERS properties of these plasmonic MoO₂ nanosheets, a confocal micro Raman spectrometer (LabRAM HR Evolution) is used as the characterizing instrument. In all SERS detections, the adopted excitation wavelength is 532 nm and the laser power is 0.5 mW, and the magnification of the objective is $\times 50$ L. R6G aqueous solutions with concentration varied from 10⁻⁴ to 10⁻⁷ M were obtained from a stock solution of 10⁻³ M by successive dilution and then were used as the probe molecules. To improve the signal reproducibility and uniformity, the MoO₂ nanosheets were dipped into a probe solution to be measured for 20 min, then taken out and dried in air for 1 h. In all SERS detections, the laser beam is perpendicular to the top of the sample to be tested with a resultant beam spot diameter of 5 μ m.

4. Calculation:

The first-principles calculations were carried out with CASTEP, which employed the density functional theory plane-wave pseudopotential method with the Perdew-Burke-Ernzerhof exchange-correlation function. The electron-ion interactions were described by the ultrasoft pseudopotentials (USPPs). For the simulation supercells, 4*2*1 k-point mesh was applied to sample the Brillouin zone, while 4*4*4 k-point mesh was applied for the unit cells of MoO₂ and MoO₃ to ensure the accuracy of calculation results. The self-consistent field calculation was kept within the energy convergence criterion of 1 \times 10⁻⁶ eV/atom. In addition, the Tkatchenko-Scheffler scheme was used for DFT-D correction to better describe the non-bonding interaction. As shown in Fig. S6, the highest occupied states of MoO₃ are mostly composed of O 2p orbitals, and the conduction band is dominated by Mo 3d states with some hybridization with O 2p

states, resulting in a band gap of ~ 1.75 eV. In contrast, the region near the Fermi level of MoO_2 is composed of Mo3d orbitals, exhibiting a metallic character rather than semiconducting properties.

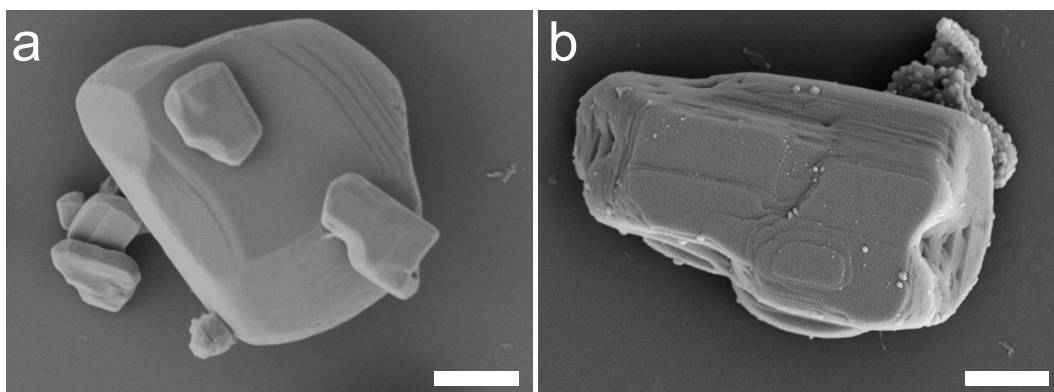


Fig. S1. SEM images of the bulk MoO₃ crystals before (a) and after (b) thermal treatment with Zn powder for 0.5 h. Scale bars are 1 μm .

As shown in Fig. S1, the layered morphology of MoO₃ crystals was well preserved after the thermal treatment, indicating that only the very top surface of the bulk MoO₃ crystals converted into MoO₂. This atomically thin product is considered as a naturally formed 2D material.

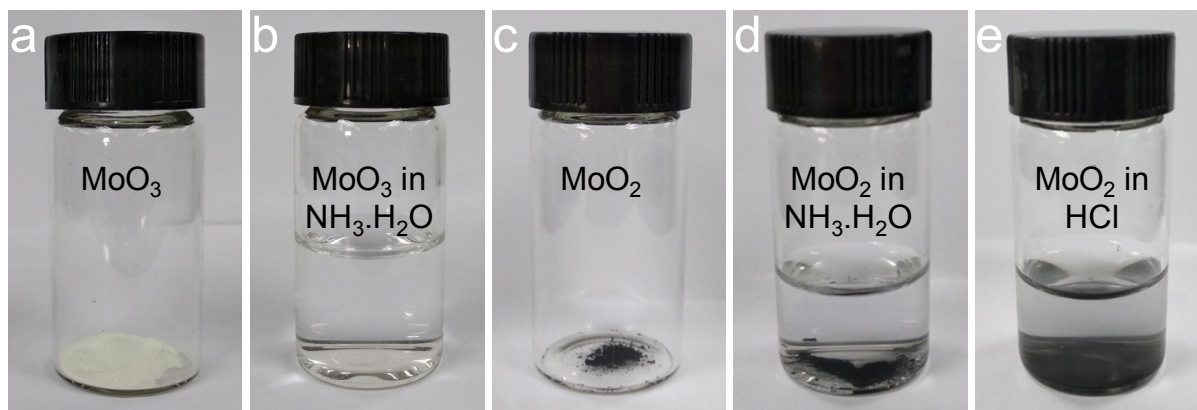


Fig. S2. Photograph of the commercial MoO_3 powder (a), MoO_3 powder in $\text{NH}_3\cdot\text{H}_2\text{O}$ (b), commercial MoO_2 powder (c), MoO_2 powder in $\text{NH}_3\cdot\text{H}_2\text{O}$ (d) and MoO_2 powder in HCl aqueous solution (e).

As shown in Fig. S2a-d, MoO_3 powder was completely dissolved in the $\text{NH}_3\cdot\text{H}_2\text{O}$ solution while MoO_2 powder can be well preserved. Besides, MoO_2 also show ultrahigh stability in HCl aqueous solution (Fig. S2e). Thus, we can use $\text{NH}_3\cdot\text{H}_2\text{O}$ and HCl aqueous solution to exclude the unreacted MoO_3 crystals and Zn powder, respectively.

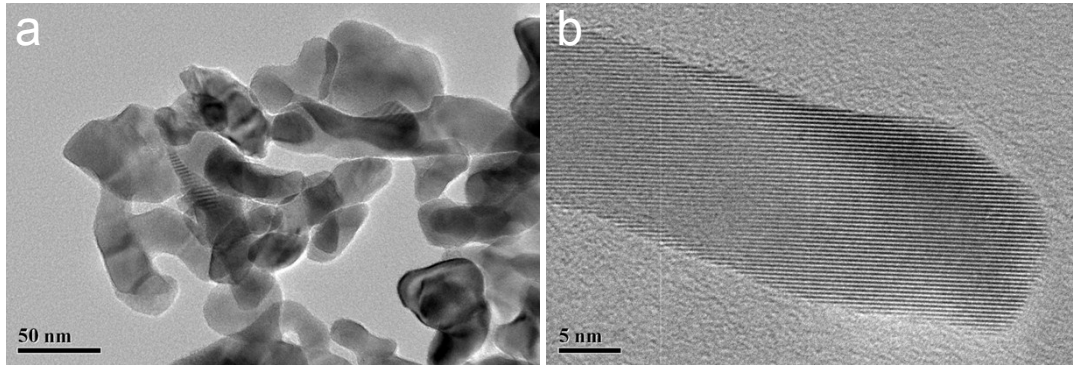


Fig. S3. TEM and the HRTEM images of the as-prepared MoO₂ nanosheets

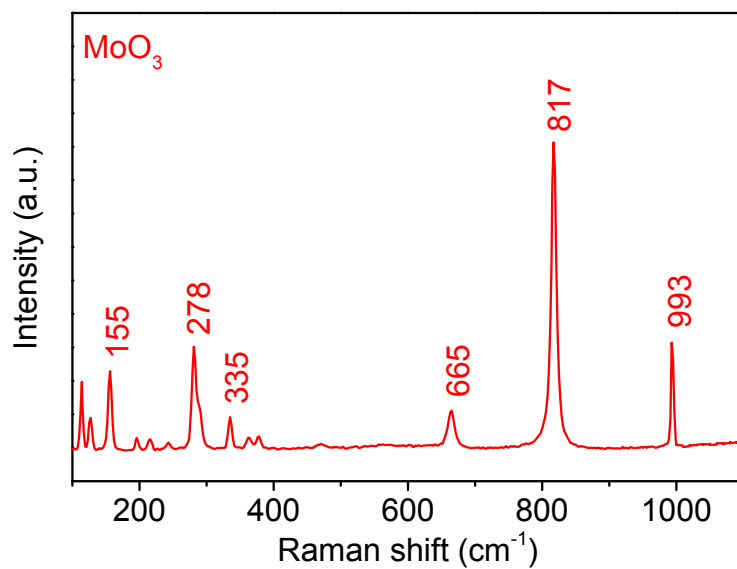


Fig. S4. Raman spectrum of the MoO₃ crystals.

As shown in the Fig. S4, MoO₃ crystals exhibit Raman scattering peaks at 155, 278, 335, 665, 817 and 993 cm⁻¹, which is distinct different with the as-prepared 2D nanosheets.

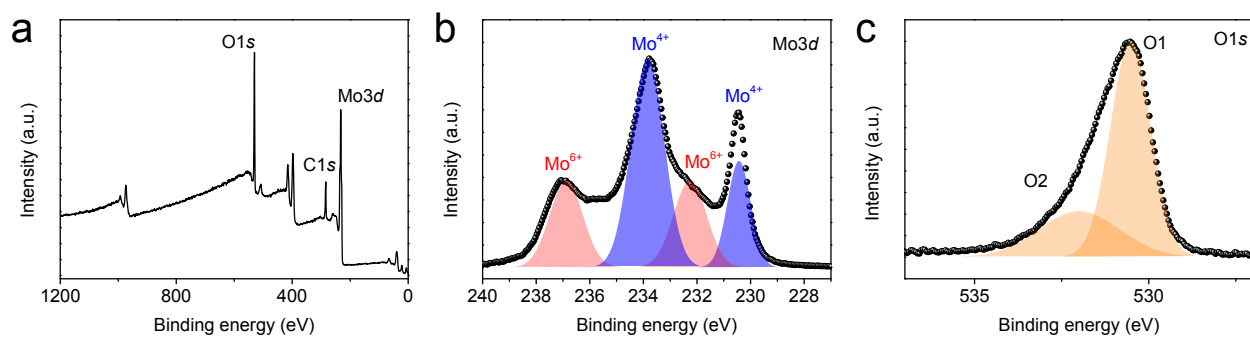


Fig. S5. (a) Survey XPS spectra of the commercial MoO₂ powder. The corresponding high-resolution Mo 3d spectrum (b) and O 1s spectrum (c).

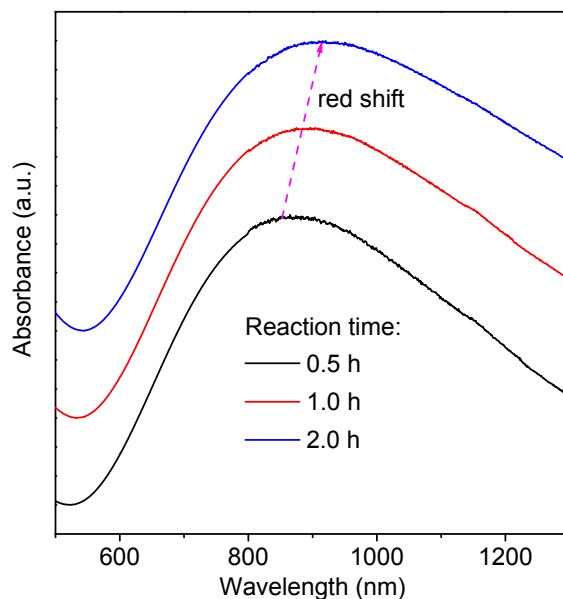


Fig. S6. Ultraviolet-vis absorption spectra of the sample obtained from different reaction time: (a) 0.5 h; (b) 1.0 h; (c) 2.0 h.

According to the proposed growth mechanism (Fig. 1a in the main text), the thickness of the 2D MoO₂ nanosheets is in direct proportion to the reaction time. Thicker nanosheets would be obtained when we prolong the reaction time. As shown in Fig. S6, the absorption peak of the as-prepared 2D MoO₂ nanosheets exhibits a distinct red-shift with increasing the reaction time, suggesting that the absorption peak was sensitive to the thickness of the samples, which is a typical feature of the localized surface plasmon resonance.

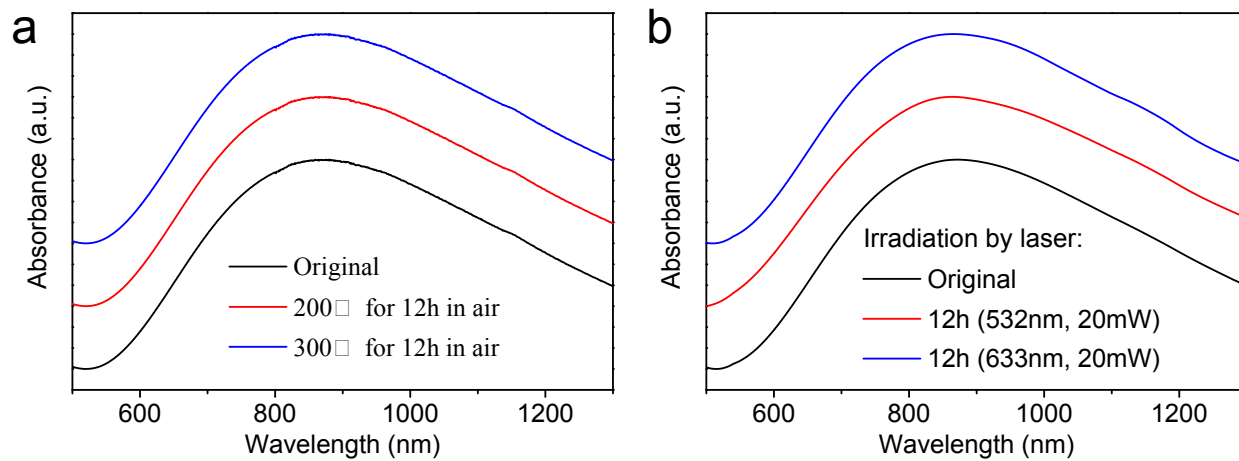


Fig. S7. The absorption peak of the 2D-MoO₂ nanosheets are almost the same after being heated in air (a) and irradiated by laser (b), suggesting the high stability of the MoO₂.

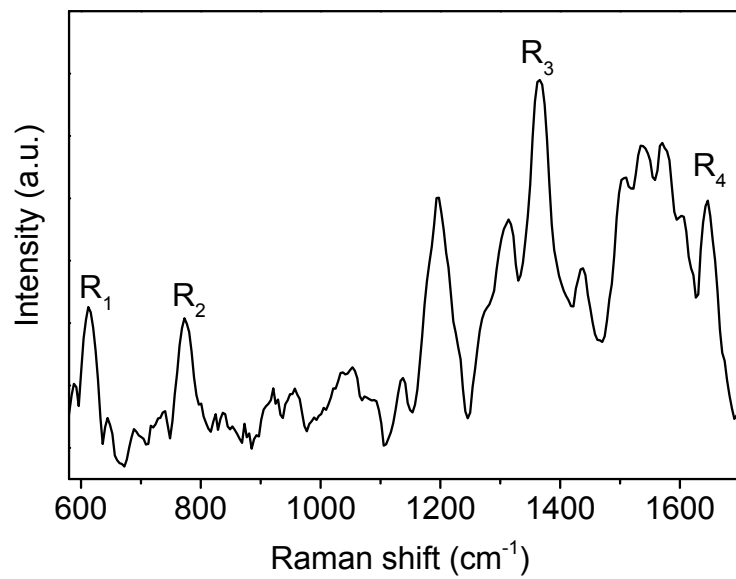


Fig. S8. Raman spectra of 10⁻³ M R6G aqueous solution.

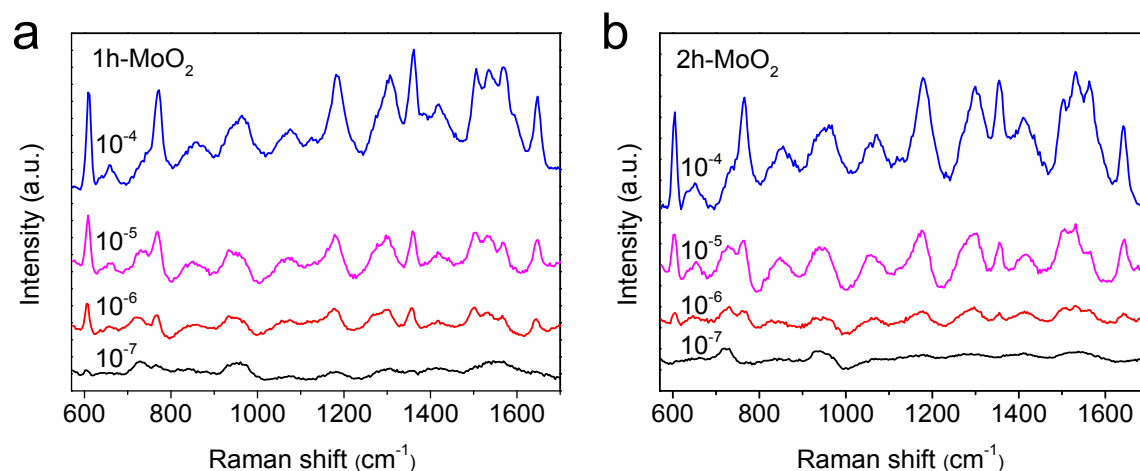


Fig. S9. SERS spectra of 2D MoO₂ nanosheets obtained from different reaction time: (a) 1.0 h and (b) 2.0 h.

According to the proposed growth mechanism (Fig. 1a in the main text), the thickness of the 2D MoO₂ nanosheets is in direct proportion to the reaction time. Thicker nanosheets would be obtained when we prolong the reaction time. As shown in Fig. S9, the Raman signal enhancement of the MoO₂ nanosheets obtained at 1h (1h-MoO₂) is obviously larger than that of the 2h-MoO₂. Furthermore, when the dye concentrations reduced to 10⁻⁷ M, identifiable Raman signal (characteristic peak at 612 cm⁻¹) was observed on the 1h-MoO₂ substrate (Fig. S9a) while the no SERS spectra of Rh6G were obtained on the 2h-MoO₂ (Fig. S9b).

Table S1. SERS property comparison with previous works based on the semiconductor substrates.

Substrate	Probe molecule	Limit of detection (M)	Literature source
WO_{2.72}	R6G	10 ⁻⁷	Nat. Communications , 2015, 6, 7800.
MoS₂	R6G	10 ⁻⁷	Nat. Communications. 2017, 8, 1993.
MoO₂ (dumbbell-like nanostructures)	R6G	10 ⁻⁷	Nat. Communications, 2017, 8, 14903.
H_xMoO₃	R6G	10 ⁻⁸	Small, 2018, 14, 1801523.
1T'-WTe₂ (MoTe₂)	R6G	10 ⁻¹⁵ (10 ⁻¹⁴)	J. Am. Chem. Soc. 2018, 140, 8696-8704.
2D-MoO₂	R6G	10 ⁻⁷	This work

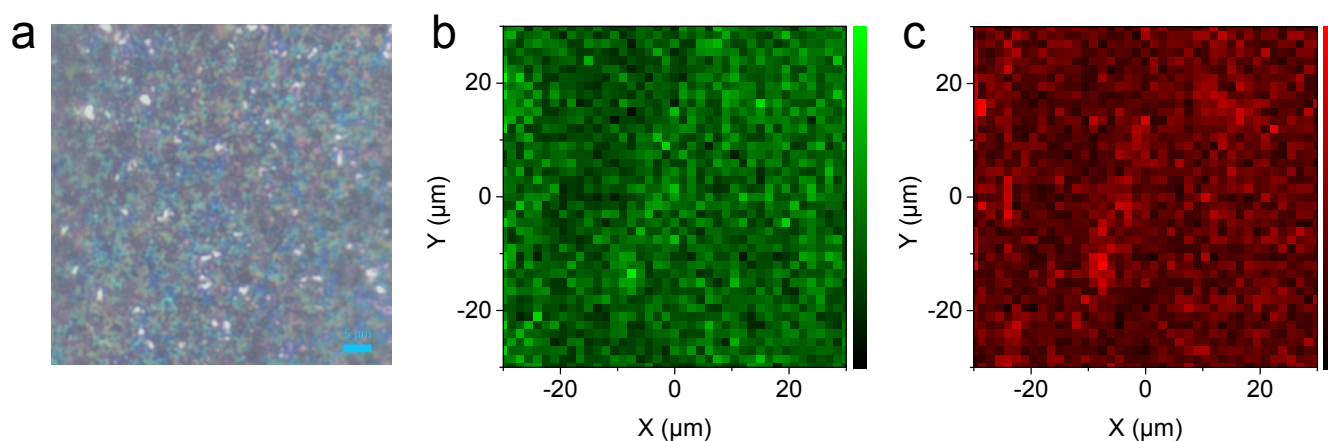


Fig. S10. Demonstration of the signal uniformity of the 2D-MoO₂ SERS substrate. (a) Optical photograph of the 2D-MoO₂ SERS substrate. The SERS mapping at 612 cm⁻¹ (b) and 773 cm⁻¹ (c) of 10⁻⁶ M Rh6G in the region shown in a.

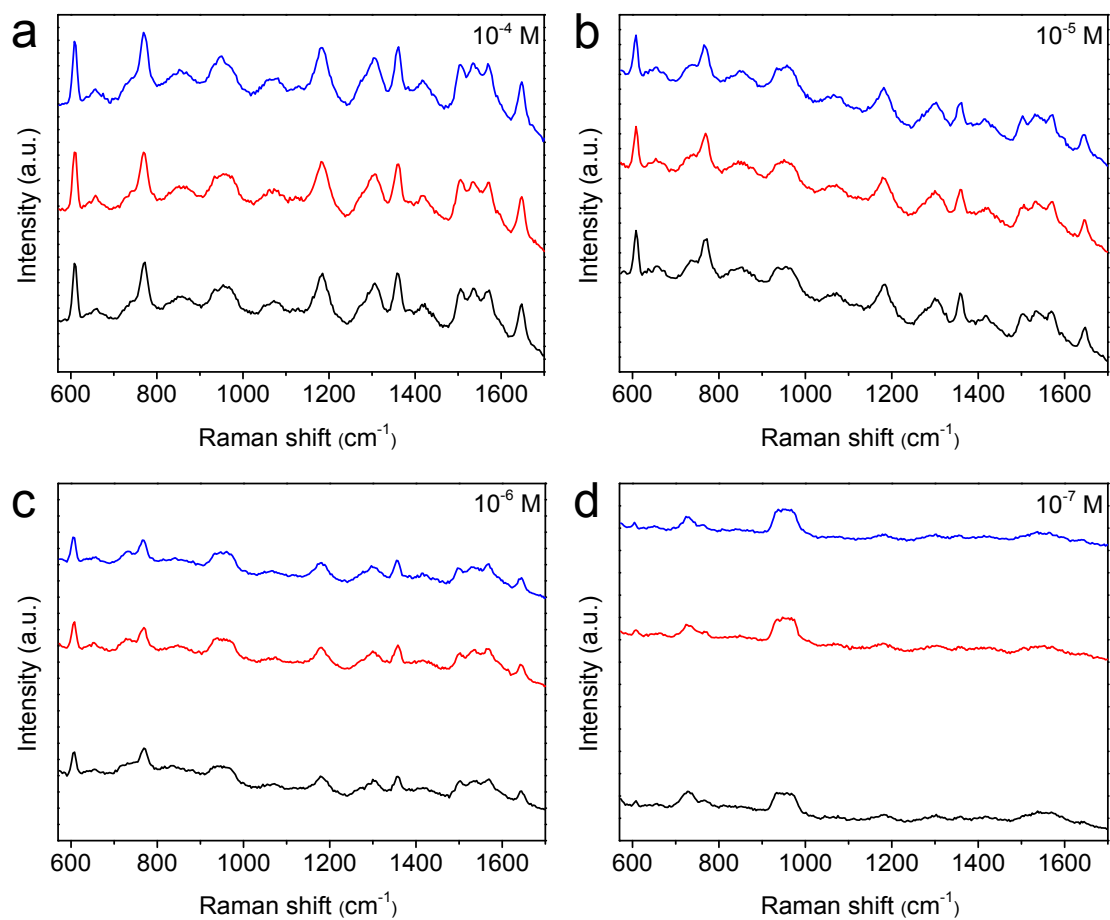


Fig. S11. SERS spectra of three different batch 2D-MoO₂ samples (black, red and blue lines) with various concentrations from 10⁻⁴ to 10⁻⁷ M (a-d).

As shown in Fig. S11, the SERS spectra collected from three different batch samples coincide well with each other, indicating that the Raman enhancement is repeatable among different 2D-MoO₂ samples.

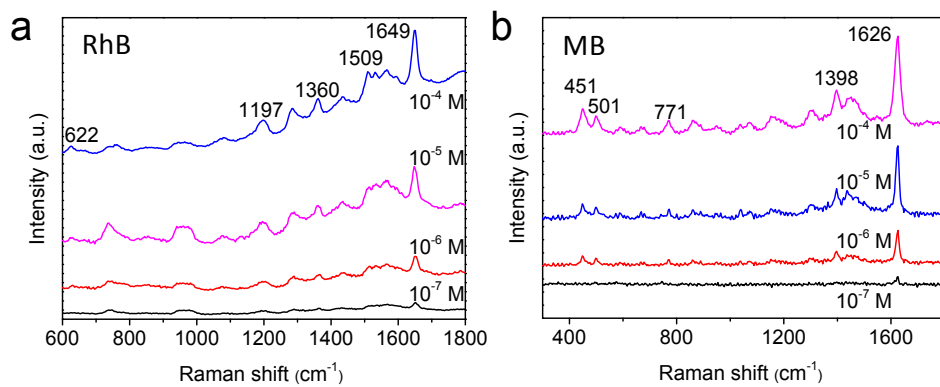


Fig. S12. Demonstration of the universality of the 2D-MoO₂ SERS substrate. SERS spectra of the rhodamine B (a) and methylene blue (b) coated on 2D-MoO₂ nanosheets with various concentrations from 10⁻⁴ to 10⁻⁷ M.